

# PRELIMINARY TRAJECTORY DESIGN METHOD FOR CONTINUOUS THRUST SYNERGETIC MANEUVERS FOR PLANETARY FLYBYS

Ghanghoon Paik\*, Robert G. Melton<sup>†</sup>

A solution to Lambert's problem gives the required delta-v to transfer from one point to another in a given time of flight. The porkchop plot is a set of Lambert's solutions (delta-v's) within a given range of dates which provides windows of launch or arrival dates. A series of Lambert's solutions can be used to generate a sequence for multiple planetary visits. In addition to continuous thrust during the flyby phase, layers of porkchop plots can be combined for path planning. This paper introduces an idea to design a gravity assist mission trajectory with applied continuous thrust synergetic maneuvers at the planetary encounters.

## INTRODUCTION

Numerous spacecraft have entered orbit around Jupiter and Saturn, or have left the solar system, after using one or more gravity assists (flybys). Such maneuvers reduce the amount of propellant required for the mission, but require precise timing that is dictated by the celestial mechanics of the planets. The first gravity assist was performed by Luna 3 in 1959 and the technique has subsequently been widely applied to missions such as Pioneer, Voyager, Galileo and Cassini. A gravity assist permits a spacecraft to observe larger celestial objects relatively closely while also benefiting from the gravitational interaction to change the magnitude and/or direction of its velocity.<sup>1-4</sup> In order to maximize the energy gain from a flyby maneuver, thrust can be applied to dramatically change the delta-v.<sup>5-7</sup> This combination of gravity assist and propulsive thrust is known as a synergetic maneuver.

Since the gravity assist maneuver is an effective tool for steering a spacecraft, it can be used to expand scientific opportunities (e.g., observe planetary moons during a flyby). Previous work has considered the use of combined impulsive thrust and gravity assists, as well as the use of impulsive or continuous thrust for interplanetary trajectory correction maneuvers.<sup>8-17</sup>

The main purpose of the research is to develop an algorithm that can easily plan out the schedule for multiple gravity assists and to understand the influence of additional continuous thrust during the planetary flyby. This research work is still in progress and only available to show the progress at this stage. Currently, graphically analyzing various porkchop plots is used to evaluate possible schedules and requirements. These steps are essential since they can be used as a guideline for mission planning.

---

\*PhD candidate, Department of Aerospace Engineering, Pennsylvania State University, University Park, PA 16802

<sup>†</sup>Professor, AAS Fellow, AIAA Associate Fellow, Department of Aerospace Engineering, Pennsylvania State University, University Park, PA 16802

The method introduced in this paper uses a synergetic maneuver while the spacecraft is flying inside the planet's sphere of influence (SOI), adding flexibility for planetary encounters. Also, the porkchop plots generated by multiple Lambert's solutions can provide possible transfers between planets with a given delta-v budget.

## METHODS

Gravity assist around multiple bodies requires precise targeting and scheduling. In order to find the schedule for an interplanetary mission, a porkchop plot can be used to graphically evaluate the required energy and possibilities to travel between two bodies. A porkchop plot is a contour of characteristic energies or delta-v's against departure and arrival dates. By analyzing available energy after each gravity assist, it may allow one to predict the next encounter.

### Spacecraft Dynamics

Planets in the solar system have relatively small inclinations to the ecliptic plane, between 0 and 7 degrees and an average of 2.3 degrees.<sup>2,18</sup> These orbital inclination differences can result in significant delta-v requirements for plane changes; however, this is often assumed to be insignificant for preliminary mission design. Therefore, the dynamics of motions in this research are also described in 2-D coplanar form. Since the inclinations of the orbits are not considered, the equations of motion can be represented in polar coordinate form as

$$\dot{\vec{x}} = \begin{bmatrix} v_r \\ -\frac{\mu-r}{r^2} v_\theta^2 \\ \frac{v_\theta}{r} \\ -\frac{v_r v_\theta}{r} \end{bmatrix} \quad (1)$$

where  $\vec{x} = [r, v_r, \theta, v_\theta]^T$ , with components of radial distance, radial velocity, angular displacement from  $x$ -axis, and transverse velocity, respectively.<sup>4,19</sup> To apply the effect of finite thrust to the spacecraft motion, a thrust term is added to the equation and the modified equation of motion is

$$\dot{\vec{x}} = \begin{bmatrix} v_r \\ -\frac{\mu-r}{r^2} v_\theta^2 \\ \frac{v_\theta}{r} \\ -\frac{v_r v_\theta}{r} \end{bmatrix} + \frac{T}{m} \begin{bmatrix} 0 \\ \sin \beta \\ 0 \\ \cos \beta \end{bmatrix}. \quad (2)$$

In Eqn. (2),  $T/m$  is the thrust-to-mass ratio and  $\beta$  is the thrust-pointing angle which is determined by the third-order polynomial

$$\beta = \hat{\beta}_1 + \hat{\beta}_2 t + \hat{\beta}_3 t^2 + \hat{\beta}_4 t^3. \quad (3)$$

The purpose of the work is to understanding behavior of continuous thrust and it can be simulated by using change in acceleration due to decrease in spacecraft mass. From the rocket equation, mass-flow rate can be described as

$$\dot{m} = \frac{T}{v_e} \quad (4)$$

where  $v_e$  is the exhaust velocity of the thruster. Therefore, the thrust-to-mass ratio ( $T/m$ ) at any given time,  $t$ , can be represented as

$$\begin{aligned}\frac{T}{m(t)} &= \frac{T}{m_0 - \dot{m}t} \\ &= \frac{T}{m_0 - T/v_e t}\end{aligned}\quad (5)$$

for the initial mass of the spacecraft,  $m_0$ .<sup>20</sup>

## Differential Evolution

Heuristic algorithms are widely known to provide better exploration of complex objective-function surfaces with potentially many local minima.<sup>21,22</sup> The work done in this paper uses a differential evolution (DE) algorithm. Heuristic algorithms are often problem-specific and particular algorithm may work better than others. After comparing several different algorithms, DE was selected since it shows advantageous benefits including faster convergence and lower chance of getting stuck in a local minima.<sup>20,23</sup> The DE algorithm uses a scale factor ( $F$ ) and crossover rate ( $C_r$ ) as major parameters.<sup>24,25</sup> They are selected from a given range of values but need to be adjusted empirically depending on the problem. By properly selecting values, the solution can be much more accurate or converge more rapidly. Algorithm 1 represents how the DE algorithm works. A minor modification was made from the original version to suitably find the optimal solution. If the cost function is not sufficiently converged, at every certain iteration, a portion of the population is randomized to extend the exploration phase of the search.

DE in this research is applied to find optimal thrust pointing angle and thrust magnitude during the powered gravity assist maneuver. Each member in the population has 10 different components

$$P = [\hat{\beta}_1^1, \hat{\beta}_2^1, \hat{\beta}_3^1, \hat{\beta}_4^1, N_{thr}^1, \hat{\beta}_1^2, \hat{\beta}_2^2, \hat{\beta}_3^2, \hat{\beta}_4^2, N_{thr}^2]. \quad (6)$$

In Equation (6),  $\hat{\beta}_i^j$  are coefficients from Eqn. (3) and  $N_j^j$  are thrust magnitudes before and after periapsis passage during a flyby maneuver. The cost function for this specific case is defined as

$$J = -|\Delta v_f| + \alpha|\Delta r_p| + \gamma. \quad (7)$$

In Eqn (7),  $|\Delta v_f|$  is the magnitude of the difference in final velocity and  $\Delta r_p$  is the difference in periapsis altitude with and without applied continuous thrust. The minus sign in front of first term is added to motivate the algorithm to increase  $\Delta v$  gain from powered maneuver. Also, the term  $\gamma$  is a penalty term for the cost function based on three different conditions

$$\gamma = \begin{cases} 15 & \text{if no encounter was found} \\ 10 & \text{if an encounter was found but flyby is not possible} \\ 0 & \text{if an encounter was found and flyby is possible.} \end{cases} \quad (8)$$

The maximum  $\gamma$  occurs when the spacecraft is more than 3 SOI radii away from each planet as it crosses that planet's orbit. Also, even though the spacecraft is within 3 SOI radii of the planet, if a flyby is not possible, a smaller penalty is added. The penalty multiplier  $\alpha$  of Eqn (7) is an inequality constraint that penalizes the cost function as defined in

$$\alpha = \begin{cases} 0 & \text{if } |\Delta r_p| < 10^{-3} \text{ or } r_p > 1.05 r_{pl} \\ 1000 & \text{if } |\Delta r_p| > 10^{-3} \text{ or } r_p \leq 1.05 r_{pl} \end{cases}. \quad (9)$$

---

**Algorithm 1:** Modified version of differential evolution algorithm

---

```
randomly generate initial population of size  $N_p$ ;  
choose  $F$  and  $C_r$  values;  
while solution is not converged or iteration  $k \leq 500$  do  
  for each member  $j$  in the population do  
    generate 5 distinct design points,  $r_1, r_2, \dots, r_5 \in (1, N_p)$  where  $r_1 \neq r_2, \dots, \neq r_5$ ;  
    generate random integer  $j_r \in (1, n)$ ;  
    if  $j = j_r$  or  $\text{rand}(0, 1) < C_r$  then  
       $U_j^k = x_{(j,r_1)}^k + F(x_{(j,r_2)}^k - x_{(j,r_3)}^k) + F(x_{(j,r_4)}^k - x_{(j,r_5)}^k)$ ;  
    else  
       $U_j^k = x_j^k$ ;  
    end  
    if  $f(\mathbf{U}^k) \leq f(\mathbf{x}^k)$  then  
       $\mathbf{x}^{k+1} = \mathbf{U}^k$   
    else  
       $\mathbf{x}^{k+1} = \mathbf{x}^k$   
    end  
  end  
  if  $k = 100$  and not converged then  
    replace  $N_p/2$  with random population  
  end  
end
```

---

Thus, if the difference in periapsis distance with and without powered maneuver is large, or if periapsis altitude is below safe approach distance, the cost function is heavily penalized.

### Sequence Searching

In order to perform swingby's around multiple planetary bodies, proper scheduling is required since it is critical for a spacecraft to approach close enough to be captured inside of SOI's at specific time. Since both the spacecraft and planets are moving simultaneously in different orbits, finding multiple encounters with limited resource is a challenging task. In this paper, a method that is using porkchop-like plots provides the initial guess to multi-body transfers.

Lambert's problem is a well-known method to determine a transfer orbit between two bodies from their position vectors.<sup>3,26-28</sup> It is a useful tool to be applied on a wide range of space missions. In the solution of a Lambert's problem, velocity vectors at the two end points are calculated. In case of orbit transfers, the calculated velocity gives required additional delta-v to reach the targeted position. By plotting sets of Lambert's solutions, a porkchop plot can be obtained. Though there are variations of porkchop plots, generally it refers to contours of departure/arrival dates and characteristic energy ( $C_3$  or  $v_\infty^2$ ). Instead of  $C_3$ , difference in velocity against departure date and time of flight (ToF) is used here to give graphical descriptions of launch windows.

In general, Lambert's solution has two significant solutions, the long and the short way, which are determined by the arc angle of transfer trajectory. If the traveling arc is less than 90 degrees, it is defined to be a short way, and if greater than 90 degrees, it is called as a long way. Depending on

the positions of two planets, one becomes prograde (traveling in the counter clockwise direction) and the other, a retrograde orbit (traveling in the clockwise direction), and contours of them form a porkchop shape. However, in this research, only prograde orbits are considered meaningful. Thus, half porkchop plots are generated based on prograde orbits and their required delta-v's. Due to the reasons previously mentioned, plots presented here do not look equivalent to traditional porkchop plots since they represent only prograde orbits. However, they will be also denoted as either porkchop or porkchop-like plots.

To analyze possibilities for multiple gravity assist maneuvers, porkchop-like plots need to be evaluated for each planet. Porkchop plots for the Voyager 2 mission are presented in Figure 1. These plots represent launch windows and time-of-flight for each transfer. In the figure, the grey area indicates the search window and the red marker indicates the actual mission date.<sup>29</sup> It is assumed that the initial search window is the 15 days before and after the actual date, the width of the launch window is 30 days and the height is duration of Hohmann transfer. Then, the next transfer's launch

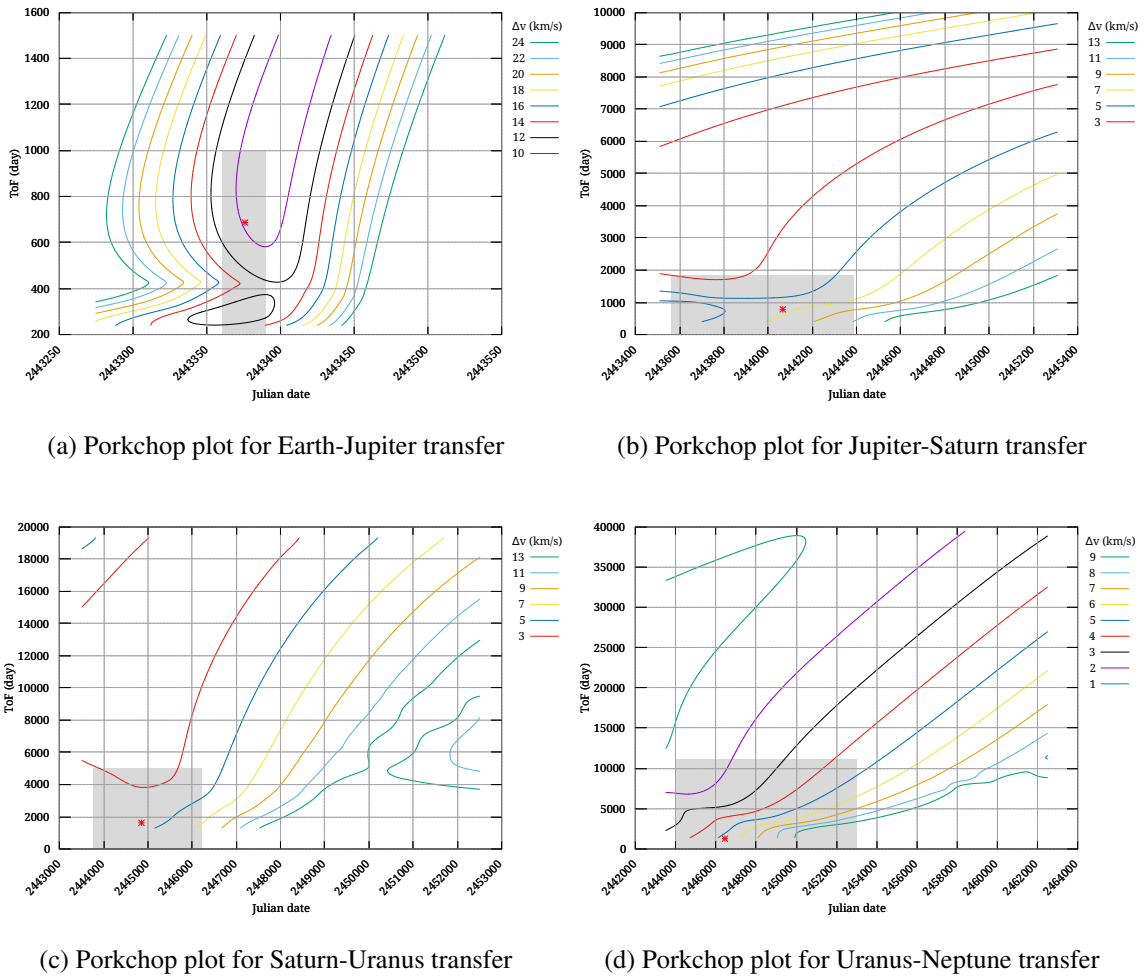


**Figure 1:** Porkchop plot for Voyager 2 mission

window is determined from the previous search window with a range of  $[date_{min} + 200, date_{max} +$

To $F_{prev}$ ]. If departing from the outer planet, half of the Hohmann time-of-flight is used to restrict the search space. As shown in the figures, all the actual mission dates lie inside the search space defined in this work. It was also verified with the Voyager 1 mission, thus, this method is assumed a valid baseline search space for mission planning.

Physical maximum  $\Delta v$  gain from planetary flyby is shown in Table 1 which is obtained from a condition where a spacecraft can fly right on the surface of a planet.<sup>1,3</sup>

Planet	Mercury	Venus	Earth	Mars	Jupiter	Saturn	Uranus	Neptune
$\Delta v$ (km/s)	3.0	7.3	7.9	3.6	42.6	25.5	15.1	16.7

**Table 1:** Physical maximum flyby delta-v from each planet

## RESULTS

It is expected that various paths from Earth to a target planet, using multiple flyby's can be found under the following assumptions: 1) mass of the spacecraft of 2000 kg, 2) the exhaust velocity of the booster of 50 km/s, 3) maximum thrust magnitude of 5 N. The required power for the spacecraft is not considered in this work and assumed to be available throughout the duration of the mission. Thrust magnitudes and pointing vectors are independently evaluated for before and after the periapsis passage.

For a maximum thrust of 5 N,  $\dot{m}$  calculated from Eqn (4) to be 0.72 kg/hr or 17.28 kg/day. Therefore, at the maximum rate, if weight of fuel is assumed to be 1000 kg, thruster can continuously burn for approximately 58 days. Since the spacecraft does not always operate with full throttle, this should be a reasonable assumption. Based on the previous results, the magnitude of thrust is less than 2 N for most of maneuvers. The thrust level is fixed at a constant level before periapsis passage, and at a (possibly different) constant level after periapsis passage. For massive planets like Jupiter and Saturn, the spacecraft has to fly for longer duration due to larger SOI radius. Thus, the spacecraft only propels when it is closer than  $0.6 r_{SOI}$  from a planet. Also, maximum thrust is limited for outer planets to avoid excessive fuel burn.

The coordinate system used for the work here is based on the ecliptic coordinate at J2000. The planetocentric coordinate axes are also aligned with the ecliptic coordinate axes. Thus, the planet's  $x$ -axis is pointing in the same direction as the heliocentric  $x$ -axis, and the planet and heliocentric  $y$ -axis' are in the same orientation, as shown in Figure 2.

Also, the minimum safe approach distance to the planet is chosen to be 5 percent of the planet's radius ( $1.05 r_{pl}$ ). Thus, the spacecraft must fly a certain altitude above the surface to avoid influence of a planet's atmosphere and the chance of collision. This restriction is implemented in a penalty to the cost function in Equation (9)

The porkchop plot similar to the Voyager 2 mission, Figure 1, is used to find a similar mission with applied continuous thrust arcs. According to the data found, Voyager 2 left Earth on August 20 1977 (JD 2443375.5), swungby Jupiter on June 9 1979 (JD 2444063.5) and Saturn on August 25 1981 (JD 2444841.5). Then, finally visited Uranus and Neptune on January 24 1986 (JD 2446454.5) and August 25 1989 (JD 2447763.5) respectively.<sup>29</sup>

Since the objective of the preliminary work in the paper is to achieve similar behavior to the Voyager missions, initial guesses are based on them. In order to generate the trajectory, it goes

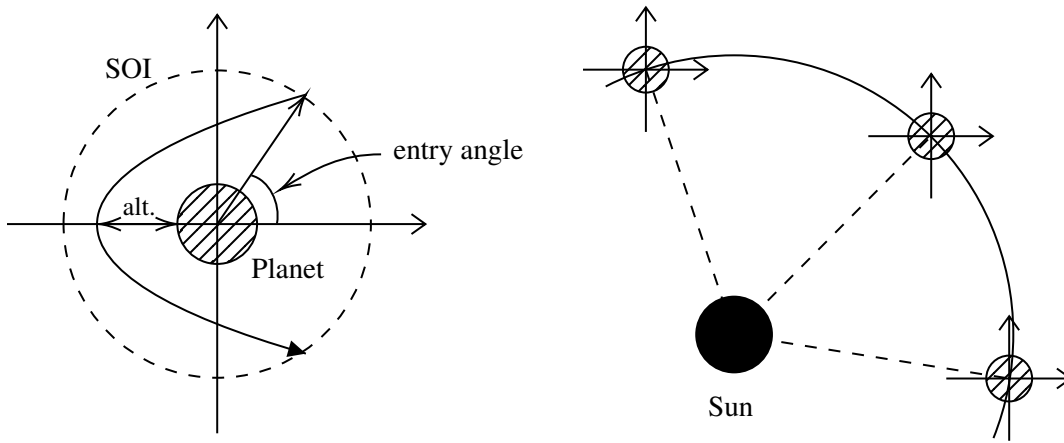


**Figure 2:** Visual description of terms and coordinate system

through several steps and is represented as a flow chart in Fig 3. Starting from the initial guess of

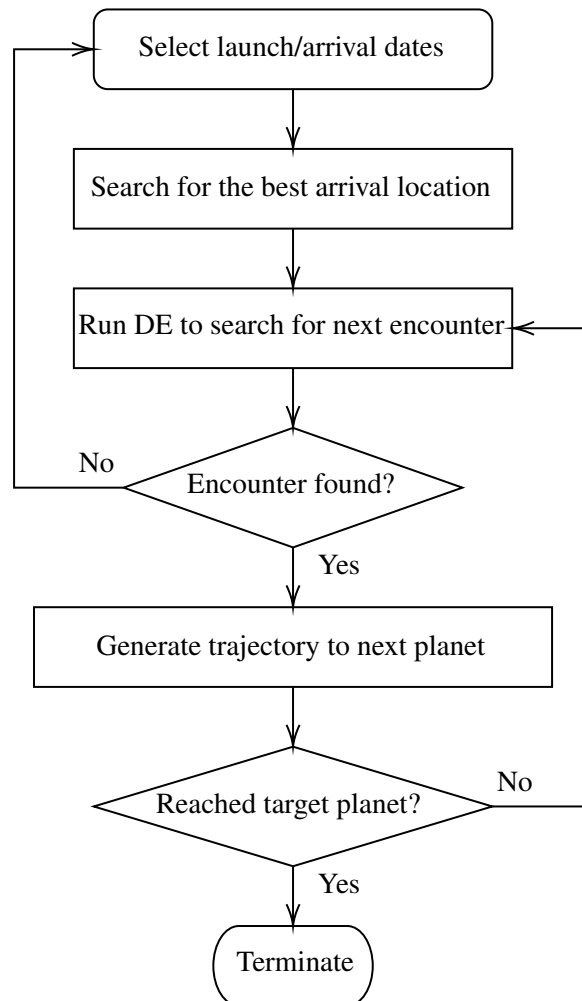


**Figure 3:** Flow chart of main steps to generate mission trajectory

launch date and arrival date, obtained from ToF, the algorithm searches for the ideal SOI arrival location of the first arrival planet. Then, differential evolution gives optimal thrust magnitude and direction. After the flyby, the next planetary encounter is searched and generates a trajectory from achieved orbital characteristics. The process terminates upon either completion of given search space or terminal condition.

Given initial guesses start with departing from the middle of year 1977 (June 1, 1977) and arriving at Jupiter around middle of year 1979 (June 1, 1979). The algorithm automatically searches from given conditions and generates multiple trajectories. One of the most successful results is presented in Figure 4 and the details for its flybys are described in Table 2. In Figure 4, an asterisk indicates position of Earth at departure, and blue and red markers indicate locations of the spacecraft at entry and exit of planet’s SOI. The figure does not attempt to present an accurate representation of the heliocentric trajectory while the spacecraft is inside the planet’s SOI. All planet locations and orbits are populated from Standish’s low accuracy model between 1800 and 2050 AD.<sup>30,31</sup>

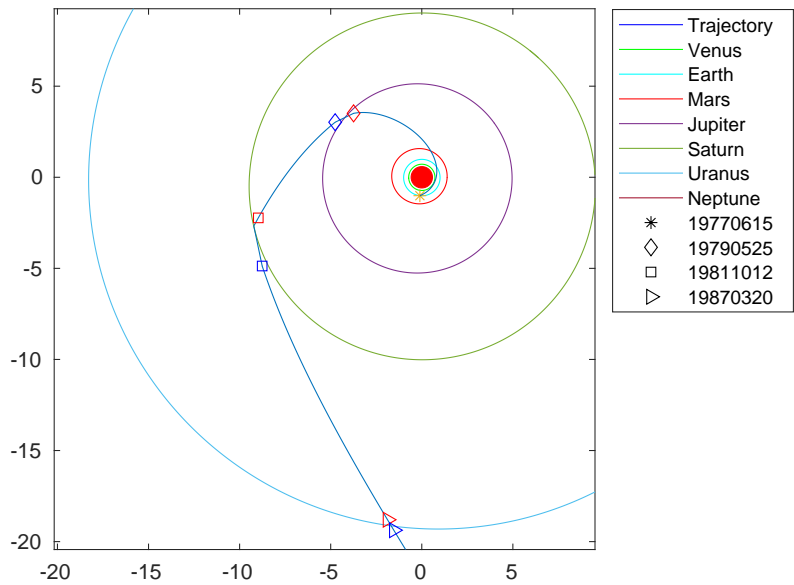


**Figure 4:** Voyager-like trajectory with gravity assist

Planet	Avg Thr (N)	$\Delta v$ (km/s)	Arr date	Dep date
Jupiter	0.6	-11.6	1979-05-25	1979-10-22
Saturn	1.5	14	1981-10-12	1983-01-02
Uranus	1	-0.1	1987-03-20	1978-05-30

**Table 2:** Specifications of powered flyby

For the preliminary results, only a Voyager-like mission trajectory is generated. However, other missions are planned to be tested to improve the algorithm, and it is expected to be able to automatically design possible multiple gravity assist missions from the given Earth launch window and delta-v budget.

## CONCLUSION

For deep space missions, it is important to understand and apply techniques to minimize fuel consumption and have a wide range of launch windows. Instead of impulsive or continuous trajectory correction maneuvers, burning fuel for relatively shorter amount of time inside SOI of planets could be a good option if it serves the purpose of the mission. The purpose of this research is to apply continuous thrust during the planetary flyby and analyze the effect of it.

Mainly, the research is focused on developing an algorithm that can automatically design a multiple gravity-assist mission. At this stage, the algorithm is compared against other missions to validate it. The algorithm still has room to be improved since it is using a less sophisticated exhaustive search method and is only partially automated its process. However, the preliminary result shows that a Voyager-like trajectory can be found. From the given window of dates, it could automatically search for trajectories with multiple planetary visits while applying continuous thrust.

As the research continues, the algorithm needs to develop more robust search algorithm. In order to improve it, systematic search algorithms including the traveling salesman problem type of method will be considered. Several other techniques such as simulated annealing and ant colonization optimization are considered to be applied as a part of search algorithm. Also, while only a forward-search method is used in this work, combining that with a backward-search is expected to generate an improved trajectory. Therefore, the final goal is a tool to design mission trajectories automatically and give options to either an extended launch window and increased number of planetary encounters.

## NOTATION

$J$	cost function
$m$	spacecraft mass
$\dot{m}$	mass flow rate
$N_{thr}$	thrust thrust magnitude
$r$	radial distance
$r_p$	radius of periapsis
$r_{pl}$	radius of planet
$T$	thrust magnitude
$t$	time
$v_r$	radial velocity
$v_\theta$	transverse velocity
$\vec{x}$	state vector
$\alpha$	penalty multiplier
$\beta$	thrust pointing angle
$\hat{\beta}_i^j$	polynomial coefficients of thrust pointing angle ( $i = 1, \dots, 4, j = 1, 2$ )
$\Delta v$	change in velocity before and after the maneuver
$\Delta r_p$	difference in periapsis distance
$\Delta v_f$	difference in final velocity (with and without thrust)
$\gamma$	planetary encounter penalty
$\theta$	angular displacement from $x$ -axis
$\mu$	gravitational parameter

## REFERENCES

- [1] A. V. Labunsky, O. V. Papkov, and K. G. Sukhanov, *Multiple Gravity Assist Interplanetary Trajectories*. CRC Press, Nov. 1998.
- [2] H. D. Curtis, *Orbital Mechanics for Engineering Students*. Butterworth-Heinemann, 3rd ed., Oct. 2013.
- [3] J. E. Prussing and B. A. Conway, *Orbital Mechanics*. Oxford University Press, 2nd ed., 2013.
- [4] B. A. Conway, ed., *Spacecraft Trajectory Optimization*. Cambridge, 2010.
- [5] H. Oberth, “Ways to spaceflight,” techreport, NASA Techdocs, TT F-622, 1972.
- [6] A. F. S. Ferreira, A. F. B. A. Prado, and O. C. Winter, “A numerical mapping of energy gains in a powered Swing-By maneuver,” *Nonlinear Dynamics*, Vol. 89, No. 2, 2017, pp. 791–818, <https://doi.org/10.1007/s1107>.
- [7] A. F. B. d. Almeida Prado and G. d. Felipe, “An analytical study of the powered swing-by to perform orbital maneuvers,” *Advances in Space Research*, Vol. 40, No. 1, 2007, pp. 102–112, <https://doi.org/10.1016/j.asr.2007.04.09>.
- [8] M. Vasile and P. D. Pascale, “Preliminary Design of Multiple Gravity-Assist Trajectories,” *Journal of Spacecraft and Rockets*, Vol. 43, No. 4, 2006, pp. 794–805, 10.2514/1.17413.
- [9] J. Englander, B. Conway, and T. Williams, “Automated Interplanetary Trajectory Planning,” *AIAA/AAS Astrodynamics Specialist Conference*, 2012.
- [10] D. H. Ellison, B. A. Conway, J. A. Englander, and M. T. Ozimek, “Analytic Gradient Computation for Bounded-Impulse Trajectory Models Using Two-Sided Shooting,” *Journal of Guidance, Control, and Dynamics*, Vol. 41, No. 7, 2018, pp. 1449–1462, 10.2514/1.G003077.
- [11] D. H. Ellison, B. A. Conway, J. A. Englander, and M. T. Ozimek, “Application and Analysis of Bounded-Impulse Trajectory Models with Analytic Gradients,” *Journal of Guidance, Control, and Dynamics*, Vol. 41, No. 8, 2018, pp. 1700–1714, 10.2514/1.G003078.
- [12] A. Gad and O. Abdelkhalik, “Hidden Genes Genetic Algorithm for Multi-Gravity-Assist Trajectories Optimization,” *Journal of Spacecraft and Rockets*, Vol. 48, No. 4, 2011, pp. 629–641.
- [13] D. Izzo, V. M. Becerra, D. R. Myatt, S. J. Nasuto, and J. M. Bishop, “Search space pruning and global optimisation of multiple gravity assist spacecraft trajectories,” *Journal of Global Optimization*, Vol. 38, June 2007, pp. 283–296.
- [14] M. Ceriotti and M. Vasile, “MGA trajectory planning with an ACO-inspired algorithm,” *Acta Astronautica*, Vol. 67, No. 9-10, 2010, pp. 1202–1217.
- [15] S. Wagner and B. Wie, “Hybrid Algorithm for Multiple Gravity-Assist and Impulsive Delta-V Maneuvers,” *Journal of Guidance, Control, and Dynamics*, Vol. 38, Nov. 2015, pp. 2096–2107, 10.2514/1.G000874.
- [16] T. T. McConaghy, T. J. Debban, A. E. Petropoulos, and J. M. Longuski, “Design and Optimization of Low-Thrust Trajectories with Gravity Assists,” *Journal of Spacecraft and Rockets*, Vol. 40, No. 3, 2003, pp. 380–387, 10.2514/2.3973.
- [17] L. Casalino, G. Colasurdo, and D. Pastrone, “Optimal Low-Thrust Escape Trajectories Using Gravity Assist,” *Journal of Guidance, Control, and Dynamics*, Vol. 22, No. 5, 1999, pp. 637–642, 10.2514/2.4451.
- [18] D. A. Vallado, *Fundamentals of Astrodynamics and Applications*. Microcosm Press, 4th ed., 2013.
- [19] A. E. Bryson and Y.-C. Ho, *Applied Optimal Control*. Hemisphere, Washington, 1st ed., 1975.
- [20] G. Paik and R. Melton, “Evaluation of Low-Thrust Synergetic Maneuvers During Planetary Flybys,” *AAS/AIAA Astrodynamics Specialist Conference*, AAS/AIAA Astrodynamics Specialist Conference, Aug. 2021.
- [21] H. Eiselt and C. Sandblom, *Heuristic Algorithms. In Integer Programming and Network Models*. Springer, 2000.
- [22] J. S. Arora, *Introduction to Optimal Design*. Academic Press, 3rd ed., 2017.
- [23] G. Paik and R. Melton, “Low-thrust Multiple Gravity Assist Missions,” *AAS/AIAA Astrodynamics Specialist Conference*, 2020.
- [24] R. Storn, “On the Usage of Differential Evolution for Function Optimization,” *Proceedings of North American Fuzzy Information Processing*, 1996, pp. 519–523, 10.1109/NAFIPS.1996.534789.
- [25] R. Storn and K. Price, “Differential Evolution – A Simple and Efficient Heuristic for global Optimization over Continuous Spaces,” *Journal of Global Optimization*, Dec. 1997, p. 341–359.
- [26] D. Izzo, “Revisiting Lambert’s problem,” *Celestial Mechanics and Dynamical Astronomy*, Vol. 121, No. 1, 2015, pp. 1–15, <https://doi.org/10.1007/s10569-014-9587-y>.

- [27] C. Bombardelli, J. L. Gonzalo, and J. Roa, "Approximate Analytical Solution of the Multiple Revolution Lambert's Targeting Problem," *Journal of Guidance, Control, and Dynamics*, Vol. 41, No. 3, 2018, pp. 792–801, <https://doi.org/10.2514/1.G002887>.
- [28] R. P. Russell, "On the solution to every Lambert problem," *Celestial Mechanics and Dynamical Astronomy*, Vol. 131, Nov. 2019, pp. 1–33, <https://doi.org/10.1007/s10569-019-9927-z>.
- [29] O. Lutz, "Then There Were Two: Voyager 2 Reaches Interstellar Space," <https://www.jpl.nasa.gov/edu/news/2018/12/18/then-there-were-two-voyager-2-reaches-interstellar-space/>, Dec. 2018. Accessed: August 20, 2022.
- [30] E. M. Standish, "Keplerian Elements for Approximate Positions of the Major Planets," techreport, JPL/Caltech, N.D.
- [31] E. M. Standish and J. G. Williams, "Orbital Ephemerides of the Sun, Moon, and Planets," Unpublished.